APPLICATION OF AN EVOLUTION PROGRAM FOR REFRIGERANT CIRCUITRY OPTIMIZATION

Piotr A. Domanski* and David Yashar
National Institute of Standards and Technology
Gaithersburg, MD, USA

Abstract

Increased concerns about climate change have emphasized the importance of air-conditioning and refrigeration systems with a high coefficient of performance (COP). The effectiveness of heat exchangers significantly influences the vapor-compression system's COP. Evolutionary algorithms provide an opportunity to optimize engineering designs of heat exchangers beyond what is typically feasible for humans.

This paper presents a summary of our past and most recent work with finned-tube heat exchangers using an evolutionary program, Intelligent System for Heat Exchanger Design (ISHED), which optimizes refrigerant circuitry. The experiments with ISHED included evaporators and condensers working with refrigerants of vastly different thermophysical properties and heat exchangers exposed to non-uniform air distributions. In all cases, ISHED generated circuitry designs that were as good as or better than those prepared manually.

Further simulations showed that the COP ranking of R600a, R290, R134a, R22, R410A, and R32 in systems with optimized heat exchangers differed from the ranking obtained using theoretical cycle analysis. In the system simulations, the high-pressure refrigerants overcame the thermodynamic disadvantage associated with their low critical temperature and had higher COPs than the low-pressure refrigerants.

Keywords: Air conditioning, COP, finned-tube, heat exchanger, optimization, refrigerant circuitry.

1. Introduction

Increased concerns about climate change have emphasized the importance of air-conditioning and refrigeration systems with a high coefficient of performance (COP). The effectiveness of heat exchangers significantly influences the vapor-compression system's COP. A multitude of design parameters, some of which are limited by the application or available manufacturing capabilities, affect the heat exchanger performance. For finned-tube heat exchangers, one of the most important parameters is the sequence in which the tubes are connected to define the flow path of refrigerant through the coil, i.e., the refrigerant circuitry. The refrigerant circuitry is typically determined after the heat exchanger's outside dimensions, tube diameter, tube and fin spacing, and heat transfer surfaces are selected.

Several studies have indicated the importance of proper design of refrigerant circuitry on heat exchanger and system performance. Granryd and Palm (2003) conducted an analytical study on the optimum number of parallel sections in an evaporator, and presented their results in terms of a drop in refrigerant saturation

* piotr.domanski@nist.gov

temperature. They concluded that for optimum operation the drop of saturation temperature should be 33 % of the average temperature difference between the refrigerant and the tube wall, although the result was dependent on the refrigerant heat transfer and pressure drop correlations. Casson et al. (2002) presented a simulation study in which they evaluated the performance of R22 alternatives in an optimized condenser and its effect on the system's efficiency. Their results showed that high-pressure refrigerants can be used more effectively with higher mass fluxes than R22 because of their small drop of saturation temperature for a given pressure drop. Liang et al. (2001) investigated six pre-selected circuitry arrangements using a simulation model. They concluded that a five percent savings in a heat transfer surface area is possible with a proper design of the refrigerant circuit.

An optimized refrigerant circuitry exploits refrigerant and air properties to maximize the heat exchanger capacity. The refrigerant circuitry determines the distribution of refrigerant through the heat exchanger, which impacts the refrigerant mass flux in individual tubes, heat transfer, pressure drop, and saturation temperature. The optimal refrigerant mass flux benefits the refrigerant heat transfer coefficient at a tolerable pressure drop penalty. Another consideration in designing a refrigerant circuit is to implement cross-counter flow heat exchange between refrigerant and air.

The large number of refrigerant properties influencing a heat exchangers' performance makes the task of designing the optimal circuitry rather difficult, and the level of difficulty increases when the inlet airflow to the heat exchanger is not uniform. Most commonly, a design engineer develops a refrigerant circuitry for a new heat exchanger guided by his/her experience and heat exchanger simulations. Several heat exchanger simulation models, public-domain and proprietary, account for the refrigerant circuitry and can be used in the refrigerant circuitry optimization, e.g., EVAP-COND (Domanski, 2007). However, the design engineer needs to perform these simulations manually, each time specifying different candidate circuitry architectures. However, the number of possible circuitry architectures is extremely large and therefore manual simulations can examine only a small portion of viable circuitries while a fully exhaustive automated search is not feasible. For example, a heat exchanger consisting of n tubes will have $n!$ possible circuitries considering designs that are limited to one inlet and one outlet. The true field is much larger, since it is possible to have multiple inlets and tubes that deliver refrigerant to more than one tube, a three-depth row heat exchanger with 36 tubes will have approximately $2 \cdot 10^{45}$ possible architectures. A guided automated search method, as implemented in ISHED (Intelligent System for Heat Exchanger Design, Domanski et. al., 2004), is therefore an attractive avenue for determining the optimal circuitry design. In this paper we summarize the work performed with ISHED including optimization of evaporators and condensers working with different refrigerants and uniform inlet air distribution, and R22 heat exchangers working with non-uniform inlet air velocity profile.

2. Genetic Algorithms and ISHED

Genetic Algorithms (GAs) are general-purpose search algorithms that are based on natural selection and natural genetics. The principle of natural selection was published by Darwin in 1859 before the mechanism of genetic inheritance was understood. The basic theories of heredity were discovered Mendel in 1865. One of the

key concepts of Mendel's theory was a discrete nature of hereditary factors. The theories formulated by Mendel were not well known and not accepted until 1900 when they were independently rediscovered by other researchers. Later, T. Morgan and his collaborators established the chromosome theory of heredity by showing that genes are located in series on chromosomes and are responsible for carrying the hereditary information (Michalewicz, 1999). GAs were developed in 1975 by J. Holland whose original interest was to study the phenomenon of adaptation in natural system and to develop software that would apply the important adaptation mechanism. Since then, GAs have been used in various fields and proven to provide robust search in complex spaces (Goldberg, 1989).

Examples of application of GAs in the HVAC&R field include research by Asiedu et al. (2000), West and Sherif (2001), and Maytal et al. (2006). In each of these studies, the authors used GA programs which applied basic GA operators, namely reproduction, crossover, and mutation.

The program used in our study, ISHED, has several features that are common for all GA programs, and it also implements a few unique concepts. Consistent with a conventional GA program, ISHED operates on one generation (population) of refrigerant circuitries at a time. A population consists of a given number (determined by the user) of circuitry designs. Each member of the population is evaluated by EVAP-COND, which simulates its performance and provides its capacity as a single numerical fitness value. The designs and their fitness values are returned as an input for deriving the next generation of circuitry designs. Hence, the implemented process is iterative, and it is repeated for the number of generations specified by the user.

The major difference between a basic GA program and ISHED is that ISHED uses two independent modules, a Knowledge-based Evolutionary Computation Module and Symbolic Learning Evolutionary Module, for generating new refrigerant circuitry architectures. The knowledge-based module does not use the GA-type operators (crossover, mutation) but rather eight refrigerant circuit-specific operators (SPLIT, BREAK, COMBINE, INSERT, MOVE-SPLIT, SWAP, INTERCROSS, NEW-SOURCE). In addition, these operators are not random, as in conventional GA, but domain knowledge-based, i.e., they only perform changes that are deemed suitable according to the domain-knowledge.

The symbolic learning-based module generates new individuals (designs) in an entirely different way, by hypothesis formation and instantiation (Michalski, 2000). When applied, it divides the members of the current population into three classes based on their fitness values (cooling capacity); "good", "bad", and "indifferent". The "good" and "bad" classes contain members of the population whose fitness are in the top and bottom 25 % of the current generation's fitness range, respectively. Then, the module examines the characteristics of both well- and poorly performing designs, and creates hypotheses in the form of attributional rules that characterize the better-performing architectures. These rules are applied to generate the subsequent population of designs.

The additional component of the ISHED scheme is the Control Module, which determines which of the two modules, the Knowledge-based Evolutionary Computation Module or the Symbolic Learning Module, is used to produce the next population. The Control Module monitors the progress of the optimization process from one generation to the next, and switches between the two modules when the population no longer improves,

both in terms of the best individual and the population overall. Additional information on ISHED is presented in Domanski et al. (2004).

3. Refrigerant Circuitry Optimization for Different Refrigerants and Uniform Air Distribution

3.1 Selected refrigerants

We applied ISHED to the task of optimizing refrigerant circuitries for six different refrigerants listed in Table 1. The selected refrigerants represent a wide range of thermophysical properties that affect heat exchanger and system performance. Differences in thermodynamic properties of the studied refrigerants can be visually recognized on a temperature-entropy diagram, as shown in Figure 1 with the entropy scale normalized for qualitative comparison. The shown two-phase domes are significantly different, which is chiefly due to different critical temperatures, molar specific heats, and polarity.

The critical temperature influences refrigerant pressure, vapor density, and the change of saturation temperature with respect to pressure drop, which are important parameters for heat exchanger design. Among transport properties, liquid thermal

Table 1. Refrigerant Information[1]

Refrigerant	Saturated Vapor Pressure[2] (kPa)	Molar Mass (g mol^{-1})	Molar Vapor Specific Heat [2,3] (J mol^{-1}K^{-1})	Safety Designation [4]	GWP[5] (100 years horizon)[6]
R600a	199.5	58.122	97.79	A3	20
R134a	374.6	102.03	94.93	A1	1320
R290	584.4	44.096	81.88	A3	20
R22	621.5	86.468	66.63	A1	1780
R410A	995.0	72.585	87.27	A1/A1	2000
R32	1011.5	52.024	69.16	A2	543

[1] All fluid properties based REFPROP (Lemmon et al., 2002); [2] correspond to 7.0 °C dew-point temperature; [3] at constant pressure; [4] (ASHRAE, 2001); [5] Global Warming Potential; [6] (Calm and Hourahan, 2001; IPCC, 2001)

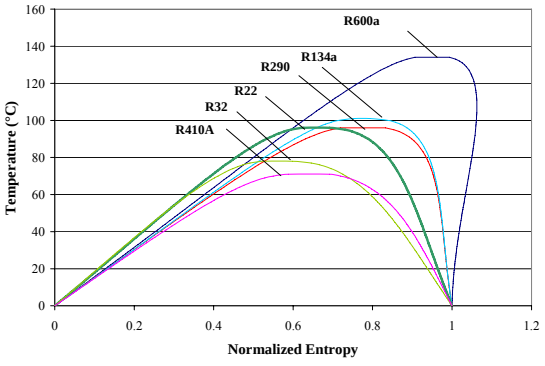

Figure 1. Temperature - Entropy diagram for studied refrigerants. (Entropy is normalized to the width of the two-phase dome.)

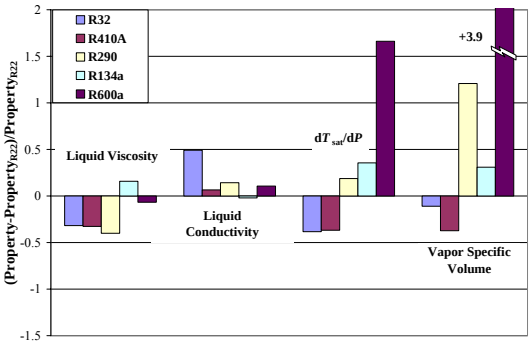

Figure 2. Thermophysical properties of selected refrigerants relative to R22 properties at 7 °C.

conductivity and liquid viscosity are the most important. Figure 2 presents these properties for the selected refrigerants relative to the corresponding properties of R22.

3.2 Evaporators optimized for different refrigerants

Table 2 shows the design data for the evaporators for which the circuitry was optimized for the selected refrigerants (Domanski et al., 2005). The evaporators used smooth copper tubes and aluminum fins. All optimizations were carried out for the air condition defined by 26.7 ºC dry-bulb temperature, 50 % relative humidity, and 101.325 kPa pressure. The refrigerant inlet condition was specified in terms of 45.0 ºC saturation temperature and 5.0 K subcooling at the inlet to the distributor. The refrigerant outlet condition was 7.0 ºC saturation temperature and 5.0 K superheat.

Table 2. Evaporator design data

Items	Unit	Value
Tube length	mm	500
Tube inside diameter	mm	9.2
Tube outside diameter	mm	10.0
Tube spacing	mm	25.4
Tube row spacing	mm	22.2
Number of tubes per row		12
Number of depth rows		3
Fin thickness	mm	0.2
Fin spacing	mm	2
Tube inner surface		smooth
Fin geometry		louver
Inlet air velocity	m s^{-1}	2.7

Before we started the optimization runs with ISHED, five basic circuitry architectures involving 1, 1→2, 2, 3, and 4 circuits were generated manually; four of them are shown in Figure 3. These circuits have optical symmetry and seemed to be appropriate designs for heat exchangers working with uniform air distribution. These circuitries were submitted as "seed" designs for the first populations used by ISHED in the optimization runs. Since one population consisted of 15 members, the remaining 11 designs of the first population were generated by ISHED. Evaporator optimization runs used 300 populations, which resulted in examination of 4500 circuitry arrangements in each optimization run.

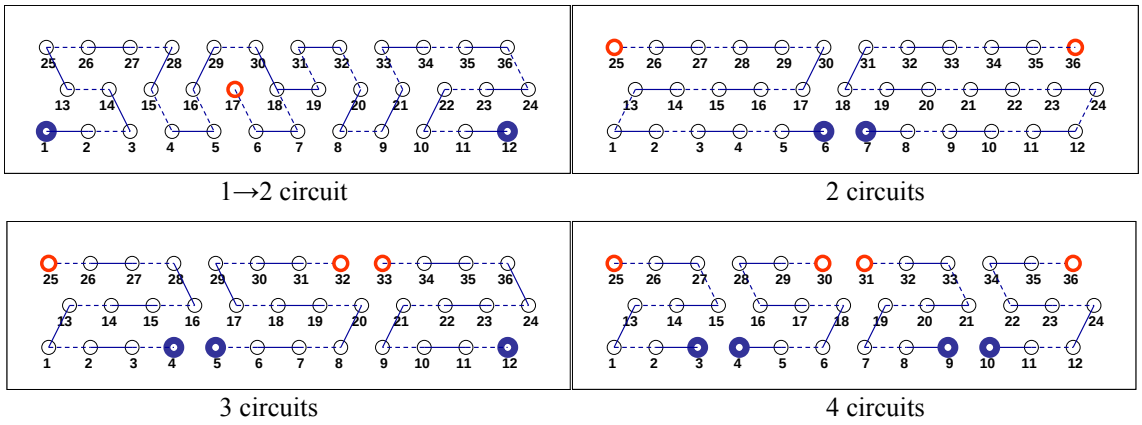

Figure 3. Manually developed 1→2, 2, 3, and 4-circuit designs (side view; circles denote tubes; solid lines indicate return bends on the near side of the heat exchanger, dotted lines indicate return bends on the far side, thick walled circles indicate inlet and outlet tubes – thicker for outlet tubes).

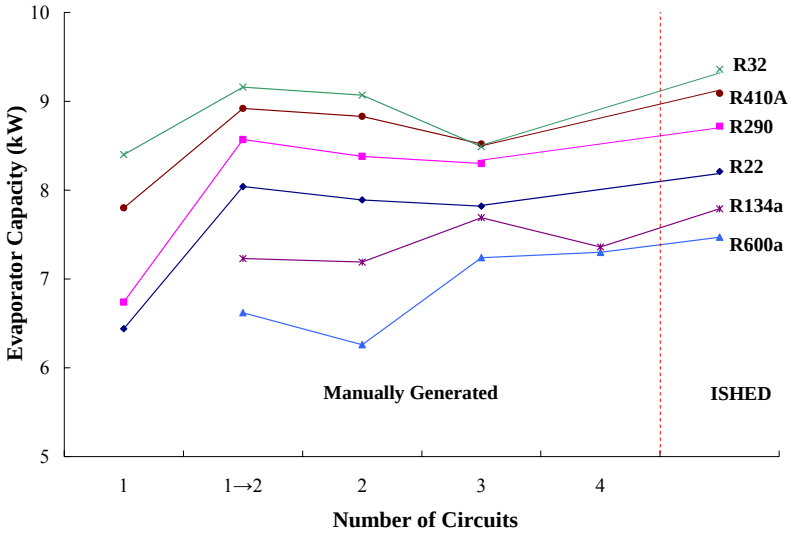

Figure 4. Evaporator capacities for manually developed and ISHED-optimized circuitry designs.

Figure 4 presents capacity results for the manually generated 1, 1→2, 2, 3, 4 circuit designs and the designs optimized by ISHED. For each refrigerant, the design developed by ISHED outperformed the best of the manually generated designs. For R32, R410A, R290, and R22, ISHED developed individually optimized designs, which were based on a 1→2 circuit. Although each of these designs had a somewhat different layout, EVAP-COND simulations confirmed that they were equivalent in performance. For this reason, only the R410A 1→2 circuitry developed by ISHED was used further for R32, R410A, R290, and R22. For R134a and R600a, ISHED proposed a 3-circuit and a 4-circuit design, respectively.

Figure 5 presents the 1→2, 3, and 4-circuit designs developed by ISHED. Among the optimized designs, R600a had the lowest capacity, 9.5 % below that of R22, and R32 had the highest capacity exceeding that of R22 by 14.5 %. We also should note that the low-pressure refrigerants, R600a and R134a, had the lowest ratio of the latent capacity to total capacity.

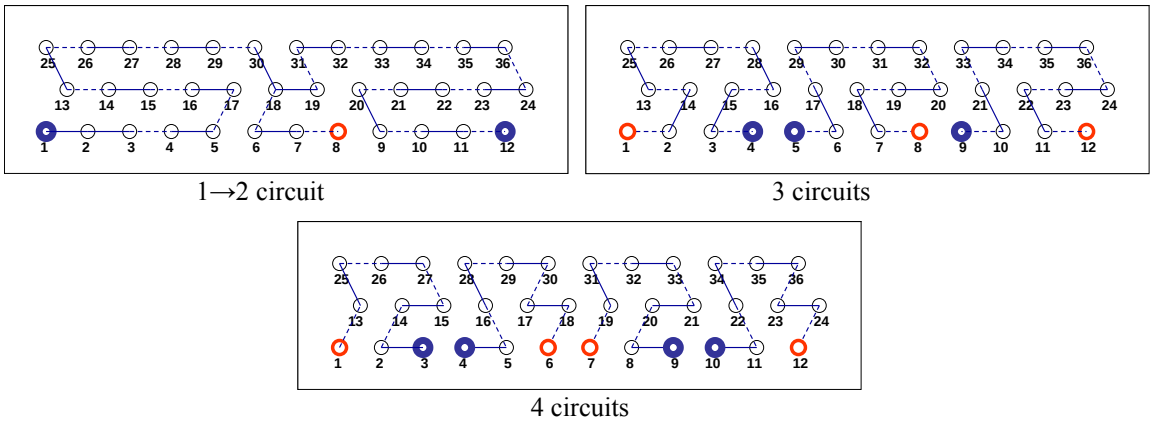

Figure 5. 1→2-circuit, 3-circuit and 4-circuit designs optimized by ISHED.

3.3 Condensers optimized for different refrigerants

Table 3 shows the design data for the condensers for which the circuitries were optimized for the selected refrigerants (Domanski and Yashar, 2007). The condensers used smooth copper tubes and aluminum fins. The air-side operating condition was defined by 35.0 ˚C inlet air temperature, 50 % relative humidity, and 101.325 kPa pressure.

The liquid subcooling at the condenser outlet was 5.0 K for each refrigerant, while the inlet condition was specified by 45.0 °C condenser saturation temperature and superheat, which was calculated for each refrigerant individually based upon evaporator exit conditions of 7.2 °C saturation temperature, 5.0 K superheat, and a compression efficiency of 0.7. This approach for determining the refrigerant state at the condenser inlet was used by Casson et al. (2002). We may note that the value of the condenser subcooling can be optimized to maximize the COP for different refrigerants working in a system; however, the resulting change in the amount of subcooling will have insignificant influence on the circuitry arrangements. Each condenser optimization run used 500 populations with 20 members per population. Hence, each single optimization run involved the generation and evaluation of 10 000 individual circuitry architectures.

Table 3. Condenser design data

Items	Unit	Value
Tube length	mm	1407
Tube inside diameter	mm	7.7
Tube outside diameter	mm	8.3
Tube spacing	mm	25.4
Tube row spacing	mm	15.9
Number of tubes per row		14
Number of depth rows		2
Fin thickness	mm	0.11
Fin spacing	mm	1.19
Tube inner surface		smooth
Fin geometry		lanced
Inlet air velocity	m s^{-1}	1.0

Before we started the optimization runs with ISHED, 14 basic circuitry architectures were manually generated. These manual designs were of five general types. They consisted of one-circuit (2 designs), 2 circuits converging to a common tube (3 designs), 3 circuits converging to a common tube (4 designs), two separate circuits (2 designs), four separate circuits (2 designs), and one design with seven separate circuits. These circuits have an optical symmetry and seemed to be appropriate designs for heat exchangers working with uniform air distribution. They were input as "seed" designs for the first populations used by ISHED in the optimization runs. Since each population consisted of 20 members, the remaining six designs of the first population were developed by ISHED.

Figure 6 shows the capacity results of the best manually designed circuit architectures and of the architectures optimized by ISHED. For R290, R22, R32, and R410A, ISHED returned circuitry designs with two circuitry branches merging at a common point. For the other remaining two refrigerants, R134a and R600a, which have a lower saturation pressure than the first group, ISHED designed circuitries with three branches merging at a common point. In each case, the ISHED design was better than or equal to the best manually designed circuitry paths.

With knowledge of the fluid properties, it seems logical that the studied fluids have the relative assortment of configurations shown in Figure 6. R600a tends to be more adversely affected by increases in mass flux, and seems to benefit from more parallel circuits than the other refrigerants. The opposite is true for R32. ISHED does not know this at the onset of the optimization run, but it learns that certain attributes tend

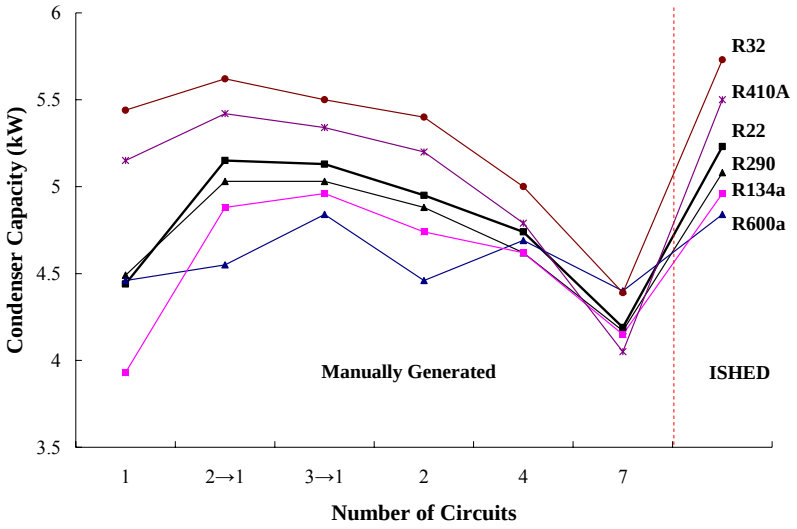

Figure 6. Condenser capacities for manually developed and ISHED-optimized circuitry designs. 2→1 and 3→1 denote 2 and 3 circuits merging to a single circuit, respectively.

to produce more favorable results and propagates these features from one generation to the next.

We may note that, although the ISHED-optimized circuitries were unique to their respective refrigerants, designs of a given type were fairly similar to one another, and each refrigerant performed approximately the same in circuitries of the same type. Figure 7 shows two designs that are characteristic of the two design groups. The designs shown were slightly modified from those generated by ISHED to accommodate manufacturing realities, e.g., elimination of overlapping return bends.

Another observation can be made that the ranking of refrigerants shown in Figure 6 corresponds to the order of their saturation pressure, i.e., the high-pressure refrigerants are better performers than the low-pressure counterparts. The capacity difference between the high-pressure R32 and low-pressure R600a is 18 %. The obtained ranking of performance agrees with the ranking obtained for evaporator optimization shown in Figure 4, with exception of the shift in relative performance of R22 and R290. This shift in ranking can be explained by a relative change in influential thermophysical properties of these fluids between the evaporating and condensing temperatures.

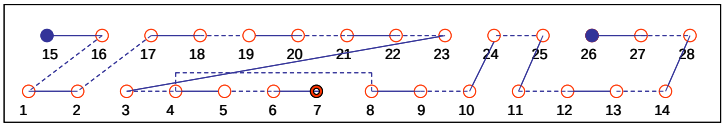

2→1 circuitry: R22, R290, R32, and R410A

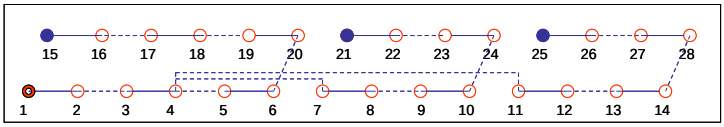

3→1 circuitry: R134a and R600a

Figure 7. ISHED-optimized circuitry designs for condensers with two and three inlets with a single outlet.

3.4 Effect of Optimized Heat Exchangers on System Coefficient of Performance

We performed simulations using our in-house detailed system simulation model of an air conditioner (ACSIM), which includes EVAP-COND models for the evaporator and condenser, to evaluate the effect of optimized heat exchangers on system efficiency. We were interested to compare the relative COP rankings of the selected refrigerants as obtained from theoretical simulations – based on the thermodynamic properties alone, as implemented by the CYCLE_D simulation program (Domanski et al., 2003) – at imposed saturation temperatures in the evaporator and condenser to the COP ranking obtained from detailed system simulations.

The ACSIM simulations were conducted at the outdoor air operating condition defined by 35.0 ˚C dry-bulb temperature, 50 % relative humidity, and 101.325 kPa pressure. The indoor air condition was 26.7 ˚C dry-bulb temperature with 50 % relative humidity and 101.325 kPa pressure. For these conditions, a reference R22 system was configured that operated with 7.0 ºC saturation temperature and 5.0 K superheat at the evaporator exit, 45.0 ºC condenser inlet saturation temperature, and 5.0 K exit subcooling. The system used the R22 optimized evaporator described in a previous section. The condenser was specially sized to satisfy the target operational criteria stated above. It used two depth rows with a total of 48 tubes, with connections that were optimized by ISHED. Once the size of R22 condenser size was determined, corresponding systems for other refrigerants were set up using the optimized evaporators presented in the previous section and individually optimized condensers having two depth rows and 48 tubes. Details regarding condenser sizing and optimization are given in Domanski and Yashar (2007).

Representation of the compression process was based on compressor maps (ARI, 2004). Specifically, compressor maps of a commercially available R22 compressor were used for the six fluids. The compressor module first calculated the refrigerant volumetric flow rate and isentropic efficiency for R22 based on the saturation temperatures at compressor suction and discharge for a system working with a specific refrigerant. Then, the compressor module calculated the refrigerant mass flow rate and compressor power for the studied refrigerant using its thermodynamic properties. The compressor module allowed the user to adjust the refrigerant mass flow rate through adjusting the compressor volumetric capacity.

The ACSIM simulations started with the reference R22 system, and were constrained by the fixed evaporator superheat and condenser subcooling that were controlled at 5.0 K. The compressor mass flow adjusting parameter was set to obtain the evaporator exit saturation temperature of 7.0 ºC. For the subsequent simulations with other refrigerants, the compressor mass flow rate was adjusted to obtain the R22 reference capacity. Depending on the refrigerant, this resulted in an increased evaporator saturation temperature and decreased condenser saturation temperature, or vice versa. Figure 8 presents the differences between the saturation temperatures in the evaporator and condenser between the studied refrigerants and R22. An increased or decreased temperature lift affected the compressor isentropic efficiency for a given case as compared to that obtained by the reference R22 system.

The theoretical CYCLE_D simulations used the R22 system saturation temperatures in the evaporator and condenser, 5.0 K evaporator superheat, 5.0 K condenser subcooling, and a compressor isentropic efficiency of 0.70. Figure 9 presents

results of the theoretical cycle simulations (CYCLE_D) and system simulations (ACSIM). For the theoretical simulations, as expected, the relative COPs of refrigerants are in descending order of their critical temperatures. For system simulations with optimized heat exchangers, the high-pressure refrigerants overcame the theoretical disadvantage and provided the highest operating efficiency. Considering that the compressor isentropic efficiency differed by less than 1 % between the studied refrigerants, the main factor responsible for the improved performance of the high-pressure fluids was the lower temperature lift of the thermodynamic cycle they realized. The low-pressure refrigerants, R600a and R134a, had a somewhat lower sensible heat ratio than the remaining refrigerants, i.e., they had a higher latent capacity.

Figure 10 provides complementary entropy generation information for the studied refrigerants. For entropy generation calculations, the expansion device and compressor were treated as adiabatic devices. The air was considered as a two-component mixture to account for the entropy change during the dehumidification process.

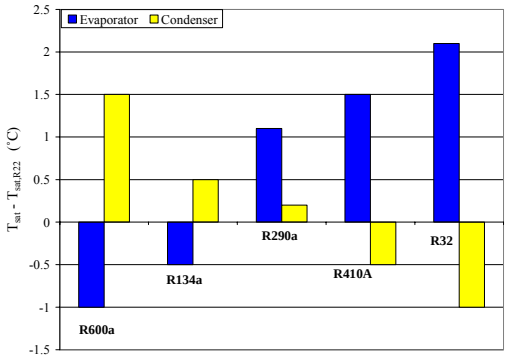

Figure 8. Differences in saturation temperature in evaporator and condenser relative to temperatures in the R22 system.

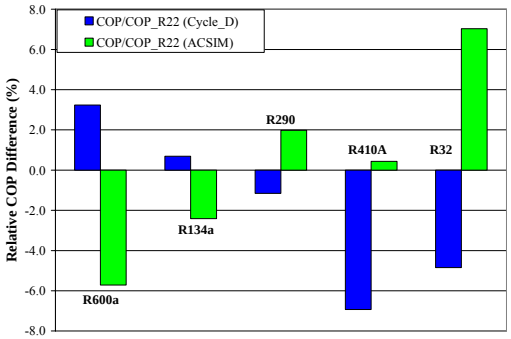

Figure 9. COP differences referenced to COP for R22 from theoretical cycle simulations using CYCLE_D and system simulations using ACSIM.

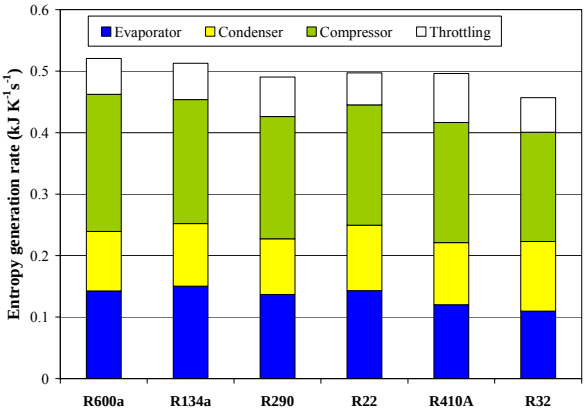

Figure 10. Entropy generation rate per 1 kW of cooling capacity.

The presented results are applicable to the system using heat exchangers where the refrigerant-side heat transfer mechanism is based on forced convection evaporation

and condensation, and are not applicable to systems with shell-and-tube type heat exchanger where pool boiling and space condensation take place. The results will vary with the variations of the relative resistances of the refrigerant and air sides.

4. Refrigerant Circuitry Optimization for Non-Uniform Air Distribution

4.1 Evaporator optimized for non-uniform air distribution

Our studies have shown that we must know the inlet air velocity profile to make informed circuitry optimization runs while designing finned-tube heat exchangers, (Domanski et al., 2004; Domanski and Yashar, 2007). Therefore, we have begun an effort to measure and predict the air flow distribution in typical residential air conditioning installation configurations. During the course of this study, we used Particle Image Velocimetry (PIV), a laser-based measurement technique, to characterize the air velocity profile at the inlet to the heat exchanger in ducted installations, and then used these measurements for comparison to Computational Fluid Dynamics (CFD) simulations of the same flow fields. In this study, we found that the air velocity profile is strongly influenced by many features within the duct, and can therefore be somewhat complicated. Here we will briefly discuss some of the results from an A-shaped coil used in our study.

We measured the approach velocity profile for an A-shaped coil with 3 depth rows and 60 tubes per heat exchanger slab. This heat exchanger has an apex angle of 34º and a metallic pan attached to the lower portion to collect condensation. The heat exchanger was installed in a straight duct in accordance with the ASHRAE test procedure (1998). The installation was horizontal for testing convenience although the field installation would be vertical. Figure 10 shows a picture of the test section.

Figure 10. Test heat exchanger for PIV measurements.

Figure 11 shows a small portion of the vector field associated with the velocity measurements; the left side of this picture corresponds to the heat exchanger inlet nearest to the condensate pan. The most interesting piece of information uncovered studying this test section is that its condensate pan acts as an airfoil, which causes a recirculation zone

in its wake. Figure 12 shows an enlarged picture from the PIV data in this region. Here we can see that the recirculation zone causes a substantial portion, approximately 1/5 of the entire heat exchanger, to receive very little air flow.

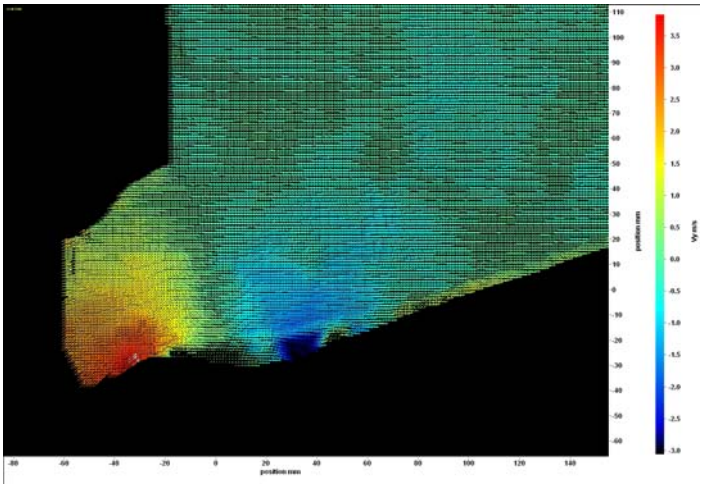

Figure 11. PIV measurements of velocity profile approaching A-shaped heat exchanger.

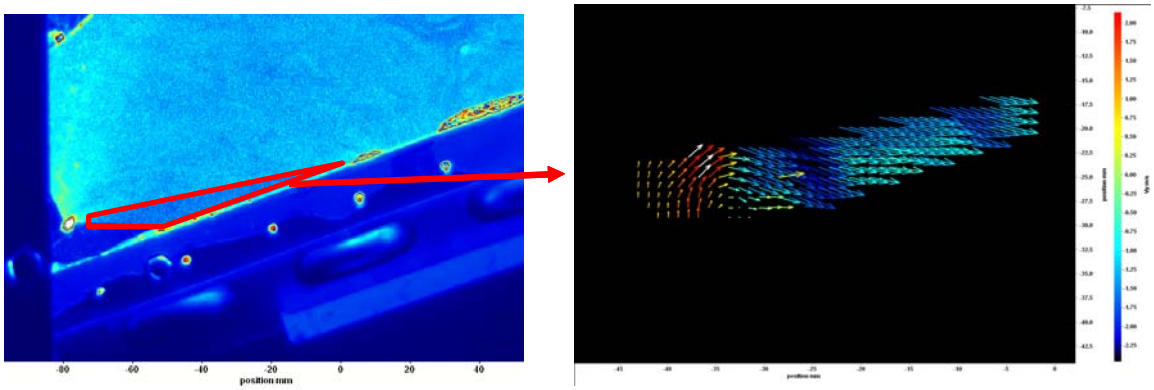

Figure 12. Recirculation zone in the wake of condensate pan on A-shaped heat exchanger.

We modeled the air flow through this heat exchanger with a commercially available CFD package, and the results agreed very well with our PIV measurements. Figure 13 presents results from our CFD simulation. Here we again focus on the recirculation zone to illustrate the velocity profile distortion caused by the presence of the condensate pan. We may note that the simulation results showed 9 of the 60 tubes in this configuration provide negligible contribution to the performance of this heat exchanger because of the lack of air flow.

We used the information found during the course of this study to redesign the tube connection sequence for this heat exchanger using ISHED and the true air velocity profile. It is important to note that the condensate pan attached to this heat exchanger is necessary to properly remove water from it, but the consequences of its presence need to be taken into consideration during design. In this case, we only examined the improvement in capacity realized by redesigning the circuitry and did not consider possible improvements from redesigning the condensate pan or heat exchanger slab. We performed EVAP-COND simulations with this evaporator working with R22, the measured air flow

distribution, and the operating conditions given in section 3.2, and then used ISHED to redesign the refrigerant circuitry. Figure 14 shows the CFD-generated air velocity profile at the heat exchanger inlet along with two circuitry options, the first being the original design, the second design is that which was obtained by ISHED resulting in a 4.2 % improvement in capacity.

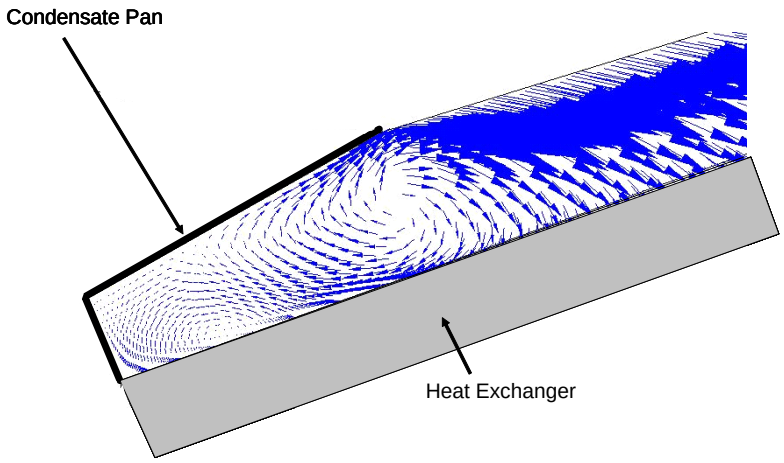

Figure 13. CFD simulation prediction of recirculation zone for A-shaped heat exchanger.

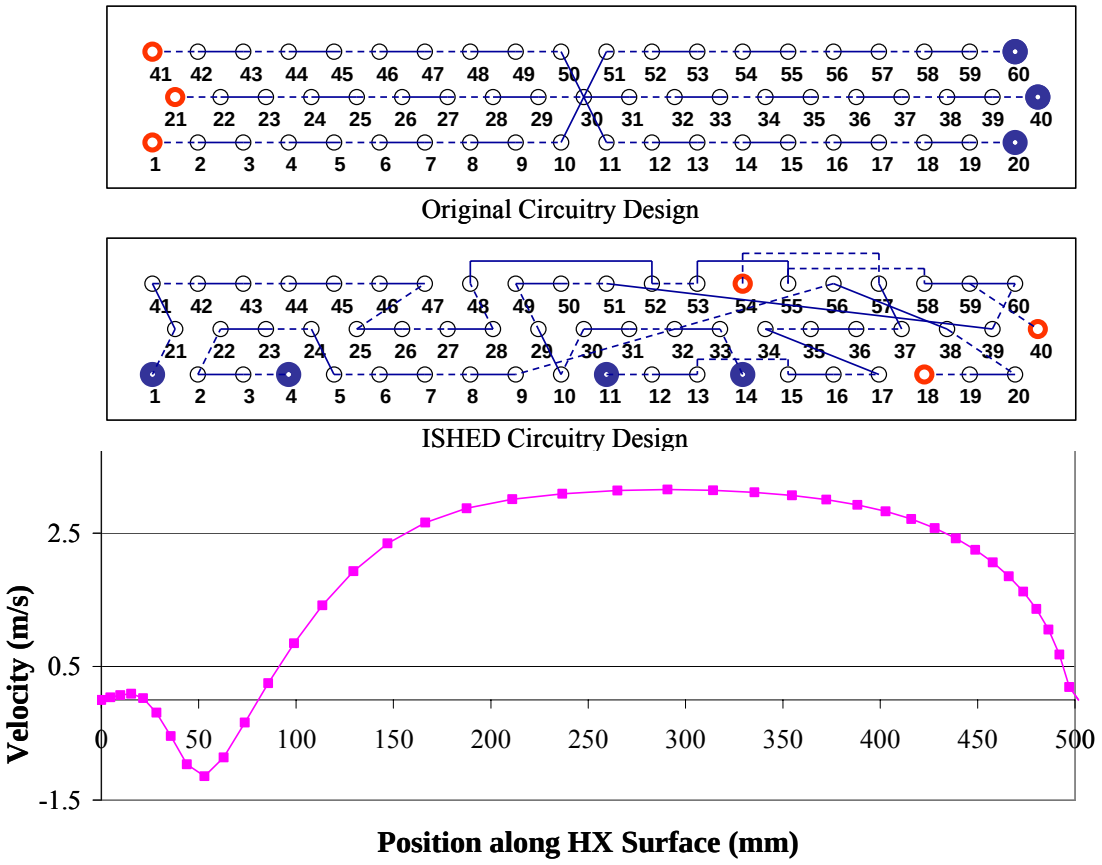

Figure 14. Original and ISHED circuitry designs with inlet air velocity profile.

4.2 Condenser optimized for non-uniform air distribution

We performed a set of simulations for an R22 condenser with a set of simple linear air velocity profiles (Domanski and Yashar, 2007). All these air velocity profiles had the same total volumetric flow rate of 0.508 $m^3 \cdot s^{-1}$, resulting in the average inlet air velocity of 1 $m \cdot s^{-1}$, but had a different height-wise velocity gradient. We defined the magnitude of this non-uniformity by the skew factor, S; S=1 for uniform air flow of 1 $m \cdot s^{-1}$, S=2 for zero flow on one side of the condenser linearly increasing to 2 $m \cdot s^{-1}$ flow on the opposite side. Other than the refrigerant circuitry, the investigated condenser was the same as those discussed in section 3.3

Figure 15 shows the capacities for the different inlet air distributions. The bottom line represents the capacities of the condenser that was optimized for the uniformly distributed air. The upper line represents the capacities of the condenser whose refrigerant circuitry was optimized for each individual air distribution. The figure demonstrates that a large portion of the capacity lost due to air flow non-uniformity can be recovered through optimized circuitry design. Hence, optimizing refrigerant circuitry becomes more important as the airflow profile becomes less uniform.

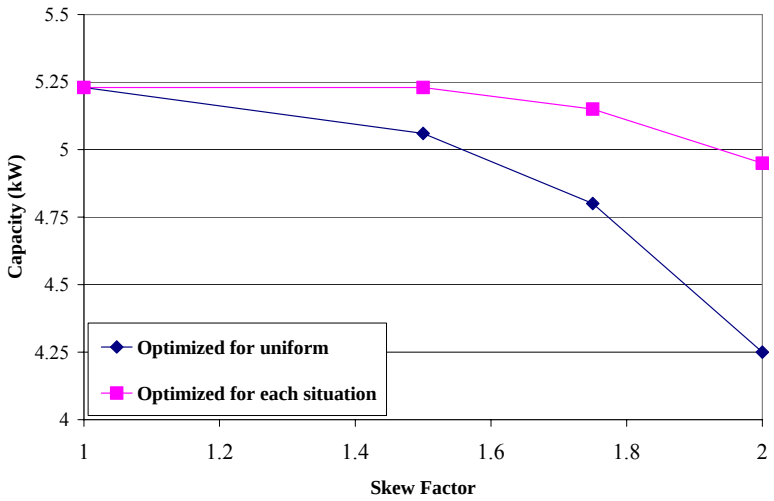

Figure 15. ISHED's recuperation of capacity loss due to non-uniform air flow.

Figure 16 presents the refrigerant circuitry design generated by ISHED for the extreme case studied, which had zero air flow at the far left side of the coil with the velocity increasing linearly to 2 $m \cdot s^{-1}$ at the right side. This design has two inlets and one outlet, but the two inlet circuits have different lengths: one circuit uses 12 tubes and the other uses 8 tubes. Even an experienced engineer would have difficulty assigning the best number of tubes per circuit and locating the merging point to maximize the coil capacity for such a non-uniform air velocity profile.

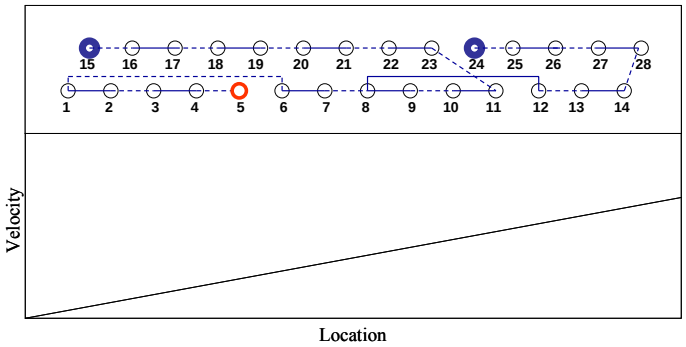

Figure 16. ISHED circuitry design for linear air flow profile.

5. Concluding remarks

We reviewed our applications of ISHED to optimizing refrigerant circuits in finned–tube evaporators and condensers. For given operating conditions and heat exchanger design constraints, the ISHED program generated optimized circuitry designs that were as good as or better than those prepared manually. ISHED-generated designs were particularly superior for operating cases with non-uniform inlet air distribution, which is more of a rule than exception. Considering that our quest for improving performance of vapor-compression systems has a limit of the Carnot cycle, and easy efficiency gains have been already taken, evolution programs like ISHED can provide the opportunity to optimize engineering designs beyond what is typically feasible for a human.

The optimization results show that the optimization process of finned-tube heat exchangers has a set of rather discreet solution options resulting in a possibility that one circuitry design may be "optimal" for more than one refrigerant. The ISHED optimization system is not constrained by the refrigerant or heat transfer surfaces used other than the limitation imposed by the heat exchanger simulator. Since the maximizing the capacity is the only objective of ISHED, it is typically required to modify manually its designs to accommodate manufacturing constrains.

The COP ranking of R600a, R290, R134a, R22, R410A, and R32 in systems with optimized heat exchangers differ from that from theoretical cycle analysis. In the system simulations, the high-pressure refrigerants overcame the thermodynamic disadvantage associated with their low critical temperature and had higher COPs than the low-pressure R134a and R600a.

References

ARI. 2004, *Performance Rating of Positive Displacement Refrigerant Compressors and Compressor Units*, Standard 540-2004, Air-Conditioning and Refrigeration Institute; Arlington, VA, USA.

ASHRAE 1998. *ANSI/ASHRAE Standard 37. Methods of testing for rating unitary air conditioning and heat pump equipment.* American Society of Heating, Refrigerating and Air-Conditioning Engineers, Atlanta, GA.

ASHRAE, 2001, *ANSI/ASHRAE Standard 34-2001; Designation and safety classification of refrigerants*. American Society of Heating, Refrigerating, and Air-conditioning Engineers; Atlanta, GA, USA.

Asiedu, Y., Besant, R.W., Gu, P., 2000, *HVAC Duct System Design Using Genetic Algorithms*, Int J HVAC&R Research; 6(2), pp. 149-174.

Calm, J.M., Hourahan, G.C., 2001, *Refrigerant data summary*. Engineered Systems; 18(11), pp.74-88.

Casson, V., Cavallini, A., Cecchinato, L., Del Col, D., Doretti, L., Fornasieri, E., Rossetto, L., Zilio, C., 2002, *Performance of finned coil condensers optimized for new HFC refrigerants*. ASHRAE Transactions; 108(2), pp. 517-527.

Domanski PA, Didion DA, Chi J. 2003, *NIST Vapor Compression Cycle Design Program − CYCLE_D*, Ver. 3.0. Standard Reference Database 49, National Institute of Standards and Technology; Gaithersburg, MD, USA.

Domanski, P.A., Yashar, D., Kaufman, KA., Michalski R.S., 2004, *Optimized design of finned-tube evaporators using learnable evolution methods*. Int J HVAC&R Research; 10(2), pp. 201-212.

Domanski, P.A., Yashar, D., Kim, M., 2005, *Performance of a finned-tube evaporator optimized for different refrigerants and its effect on system efficiency*. Int J Refrigeration; 28 (6). pp. 820-827.

Domanski, P.A., Yashar, D., 2007, *Optimization of finned-tube condensers using an intelligent system*. Int J Refrigeration; 30 (3). pp. 482-488.

Domanski, P.A., *EVAP-COND - Simulation models for finned-tube heat exchangers*, 2007, National Institute of Standards and Technology; Gaithersburg, MD, USA. http://www2.bfrl.nist.gov/software/evap-cond/

Granryd, E. and Palm, B., 2003, *Optimum number of parallel sections in evaporators*. Proceedings of the 21st International Congress of Refrigeration; Paper ICR0077, Washington, DC, USA.

Goldberg, D.E. 1989. *Genetic Algorithms in Search, Optimization, and Machine Learning*. Addison Wesley Longman, Inc.

Holland, J. 1975. *Adaptation in Natural and Artificial Systems*, University of Michigan Press, Ann Arbor.

IPCC, 2001, *Climate change 2001: The scientific basis − Contribution of working group I to the IPCC third assessment report*. Intergovernmental Panel on Climate Change of the World Meteorological Organization and the United Nations Environment Programme (UNEP); Cambridge, UK. Cambridge University Press.

Lemmon, E.W., McLinden, M.O., Huber, M.L., 2002, *NIST Reference Fluids Thermodynamic and Transport Properties Database - REFPROP*, Ver. 7.0, Standard Reference Database 23, National Institute of Standards and Technology; Gaithersburg, MD, USA.

Liang, S.Y., Wong, T.N., Nathan, G.K., 2001, *Numerical and experimental studies of refrigerant circuitry of evaporator coils*. Int J Refrigeration; 24(8), pp. 823-833.

Michalewicz, Z. 1999. *Genetic algorithms + Data structures = Evolution Programs*, 2nd extended edition, Springer-Verlag.

Michalski, R., 2000. *Learnable Evolution Model: Evolutionary Process Guided by Machine Learning. Machine Learning*; 38, pp. 9-40.

Maytal, B.Z., Nellis, G.F., Klein, S.A., Pfotemhauer, J.M., 2006, *Elevated-pressure mixed-coolants Joule-Thomson cryocooling*, Cryogenics; 46(1), pp. 55-67.

West, A.C., Sherif, S.A., 2001, *Optimization of multistage vapour compression systems using genetic algorithms. Part 2: Application of genetic algorithm and results*, Int J Energy Research, 25(9), pp. 813-824.